Molecular Traffic Control in a 3D network of single file channels and fast reactivity

Andreas Brzank^{1,3},* Sungchul Kwon², and Gunter Schütz¹

¹Institut für Festkörperforschung, Forschungszentrum Jülich, 52425 Jülich, Germany

²Department of Physics, Kyung Hee university, Seoul 130-701, Korea

³Fakultät für Physik und Geowissenschaften,

Universität Leipzig, Abteilung Grenzflächenphysik,

Linnestrasse 5, D-04103 Leipzig, Germany

(Dated: November 12, 2018)

Abstract

We study the conditions for reactivity enhancement of catalytic processes in porous solids by use of molecular traffic control (MTC) as a function of grain size. We extend a recently introduced two dimensional model system to three dimensions. With dynamic Monte-Carlo simulations and analytical solution of the associated Master equation we obtain a quantitative description of the MTC effect in the limit of fast reactivity. The efficiency ratio (compared with a topologically and structurally similar reference system without MTC) is inversely proportional to the grain diameter.

^{*}Electronic address: a.brzank@fz-juelich.de

I. INTRODUCTION

Zeolites are used for catalytic processes in a variety of applications, e.g. cracking of large hydrocarbon molecules. In a number of zeolites diffusive transport occurs along quasi-one-dimensional channels which do not allow guest molecules to pass each other [1]. Due to mutual blockage of reactands A and product molecules B under such single-file conditions [2] the effective reactivity of a catalytic process $A \to B$ – determined by the residence time of molecules in the zeolite – may be considerably reduced as compared to the reactivity in the absence of single-file behaviour. It has been suggested that the single-file effect may be circumvented by the so far controversial concept of molecular traffic control (MTC) [3, 4]. This notion rests on the assumption that reactands and product molecules resp. may prefer spatially separated diffusion pathways and thus avoid mutual suppression of self-diffusion inside the grain channels.

The necessary (but not sufficient) requirement for the MTC effect, a channel selectivity of two different species of molecules, has been verified by means of molecular dynamic (MD) simulations of two-component mixtures in the zeolite ZSM-5 [5] and relaxation simulations of a mixture of differently sized molecules (Xe and SF₆) in a bimodal structure possessing dual-sized pores (Boggsite with 10-ring and 12-ring pores) [6]. Also equilibrium Monte-Carlo simulations demonstrate that the residence probability in different areas of the intracrystalline pore space may be notably different for the two components of a binary mixture [7] and thus provide further support for the notion of channel selectivity in suitable bimodal channel topologies.

Whether a MTC effect leading to reactivity enhancement actually takes place was addressed by a series of dynamic Monte Carlo simulations (DMCS) of a stochastic model system with a network of perpendicular sets of bimodal intersecting channels and with catalytic sites located at the intersecting pores (NBK model) [9, 10, 11]. The authors of these studies found numerically the occurrence of the MTC effect by comparing the outflow of reaction products in the MTC system with the outflow from a reference system with equal internal and external system parameters, but no channel selectivity (Fig. 1). The dependency of the MTC effect as a function of the system size has been investigated in [12]. The MTC effect is favored by a small number of channels and occurs only for long channels between intersections, which by themselves lead to a very low absolute outflow compared to a

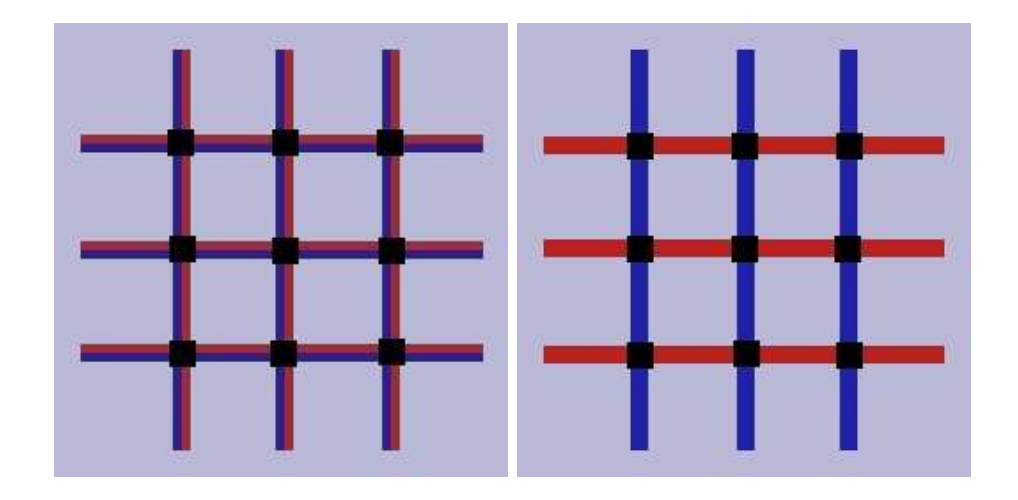


FIG. 1: REF system (left) with N=3 channels and MTC system (right) of the the same size. In contrast to the REF case, where we allow both types of particles (A and B particles) to enter any channel, in the MTC system A particles are carried through the vertical α channels whereas the B particles diffuse along the horizontal β channels. Black squares indicate catalytic sites where a catalytic transformation $A \to B$ is allowed.

similar system with shorter channels. A recent analytical treatment of the master equation for this stochastic many-particle model revealed the origin of this effect at high reactivities [13]. It results from an interplay of the long residence time of guest molecules under single-file conditions with a saturation effect that leads to a depletion of the bulk of the crystallite. Thus the MTC effect is firmly established, but the question of its relevance for applications remains open.

Here we address this question by an analytical study of the MTC system in three dimensions as a function of grain size. This may be of interest as since the first successful synthesis of mesoporous MCM-41 nanoparticles [14], there has been intense research activity in the design and synthesis of structured mesoporous solids with a controlled pore size. In particular, synthesis of bimodal nanostructures with independently controlled small and large mesopore sizes has become feasible [15].

II. NBK MODEL

Similar to [9, 12, 13] we consider the NBK lattice model as an array of $N \times N \times N$ channels (Fig. 2 left) which is a measure of the grain size of the crystallite. Each channel has L sites

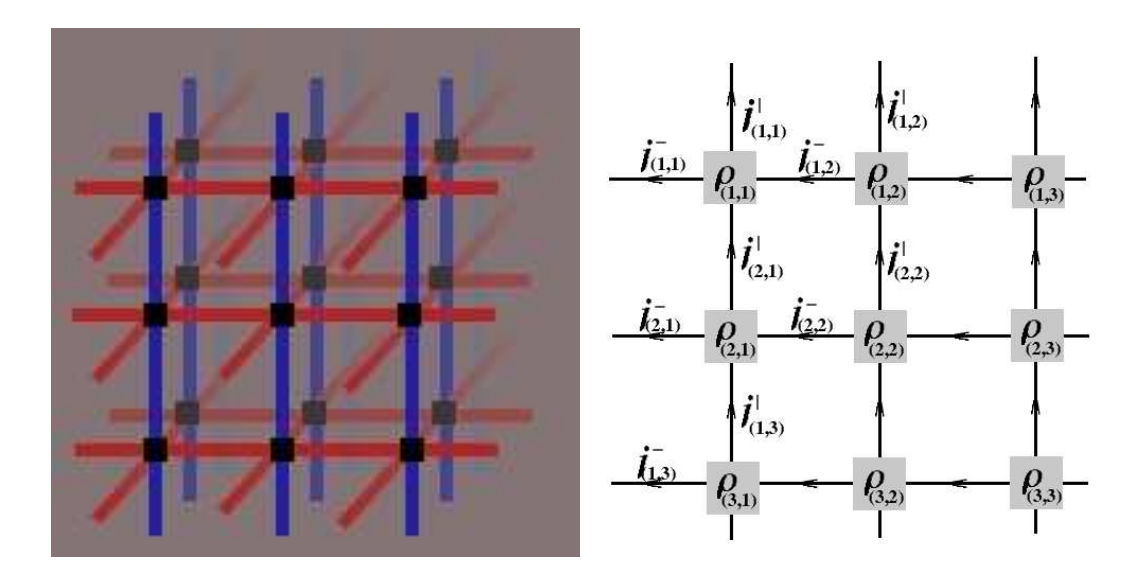


FIG. 2: (left) 3D MTC system. (right) part of the first y/z plane of β channels, view from top.

between the intersection points where the irreversible catalytic process $A \to B$ takes place. We assume the boundary channels of the grain to be connected to the surrounding gas phase, modelled by reservoirs of constant densities such that the entrances of the respective channels (extra reservoir sites) have a fixed A particle density ρ . We assume the reaction products B which leave the crystallite to be removed immediately from the gas phase such that the density of B particles in the reservoir is always 0. Short-range interaction between particles inside the narrow pores is described by an idealized hard core repulsion which forbids double-occupancy of lattice sites.

The underlying dynamics are stochastic. We work in a continuous time description where the transition probabilities become transition rates and no multiple transitions occur at the same infinitesimal time unit. Each elementary transition between microscopic configurations of the system takes place randomly with an exponential waiting-time distribution. Diffusion is modelled by jump processes between neighbouring lattice sites. D is the elementary (attempt) rate of hopping and is assumed to be the same for both species A, B of particles. In the absence of other particles D is the self-diffusion coefficient for the mean-square displacement along a channel. If a neighboring site is occupied by a particle then a hopping attempt is rejected (single-file effect). The dynamics inside a channel are thus given by the symmetric exclusion process [16, 17, 18, 19] which is well-studied in the probabilistic [20] and statistical mechanics literature [21]. The self-diffusion along a channel is anomalous, the effective diffusion rate between intersection points decays asymptotically as 1/L, see [18]

and references therein.

At the intersections the reaction $A \to B$ occurs with a reaction rate c. This reaction rate influences, but is distinct from, the effective grain reactivity which is largely determined by the residence time of guest molecules inside the grain which under single-file conditions grows in the reference system with the third power of the channel length L [18, 22]. At the boundary sites particles jump into the reservoir with a rate $D(1 - \rho_A - \rho_B)$ in the general case. Correspondingly particles are injected into the grain with rates $D\rho_{A,B}$ respectively. As discussed above here we consider only $\rho_A = \rho$, $\rho_B = 0$.

For the REF system A and B particles are allowed to enter and leave both types of channels, the blue (α) and red (β) ones (Fig. 2 left). In case of MTC A(B) particles will enter $\alpha(\beta)$ -channels only, mimicking complete channel selectivity. Therefore all channel segments carry only one type of particles in the MTC case. For the boundary channels complete selectivity implies that α -channels are effectively described by connection with an A-reservoir of density $\rho_A = \rho$ (B-particles do not block the boundary sites of α -channels) and β -channels are effectively described by connection with a B-reservoir of density $\rho_B = 0$, respectively. (A-particles do not block the boundary sites of β -channels.) This stochastic dynamics, which is a Markov process, fully defines the NBK model.

In both cases, MTC and REF system, the external concentration gradient between A and B reservoir densities induces a particle current inside the grain which drives the system into a stationary nonequilibrium state. For this reason there is no Gibbs measure and equilibrium Monte-Carlo algorithms cannot be applied for determining steady state properties. Instead we use dynamic Monte-Carlo simulation (DMCS) with random sequential update. This ensures that the simulation algorithm yields the correct stationary distribution of the model.

III. MTC IN 3D WITH LARGE REACTIVITY

Anticipating concentration gradients between intersection points we expect due to the exclusion dynamics linear density profiles within the channel segments [13, 17, 21], the slope and hence the current being inversely proportional to the number of lattice sites L. The total output current j of B particles, defined as the number of B-particles leaving the grain per time unit in the stationary state, is the main quantity of interest. It determines the effective reactivity of the grain.

We are particularly interested in studying the system in its maximal current state for given reactivity c and size constants N, L, which are intrinsic material properties of a given grain. The A particle reservoir density ρ , determined by the density in the gas phase, can be tuned in a possible experimental setting. Let us therefore denote the reservoir density which maximizes the output current by ρ^* and the maximal current by j^* . For MTC systems as defined above we always expect $\rho^*_{MTC} = 1$, since the highly charged entrances of α -channels do not block the exit of B-particles and hence do not prevent them from leaving the system.

In order to measure the efficiency of a MTC system over the associated REF system we define the efficiency ratio

$$R(c, N, L) = \frac{j_{MTC}^*}{j_{REF}^*} \tag{1}$$

which is a function of the system size N, L and reactivity c.

Let us now discuss the fast reactivity case. The penetration of A particles is controlled by c and in the limit of $c \to \infty$ A particles entering the system will be converted as soon as they reach the first intersection. Therefore, only the first and the last plane of β -channels contribute to the B particle output. The profile as well as the B particle output is fully determined by the intersection densities $\rho_{(x,y)}$. Fig. 2 (right) shows the top view of the first plane indicating our notation of the densities and currents. α -channels point into the plane and are not displayed. The current of an α -channel segment connecting the reservoir with intersection $\rho_{(x,y)}$ is denoted by $j_{(x,y)}^A$. For an analysis of the Master equation for this process we neglegt correlations between the occupancy of a catalytic site and its five neighbours. This mean field approximation is motivated by exact results for the correlations in the stationary state of the symmetric exclusion process from which it is known [21] that nearest neighbour correlations in the vicinity of the boundary of a system of size L are of order $1/L^2$. Within mean field we replace joint probabilities $\langle xy \rangle$ by the product $\langle x \rangle \langle y \rangle$. For the stationary state we identify the following currents,

$$j_{(x,y)}^{A} = D \frac{\rho \left(\rho_{(x,y)} - 1\right)}{L\left(\rho_{(x,y)} - 1\right) - 1} \tag{2}$$

$$j_{(x,y)}^{-} = D \frac{\rho_{(x+1,y)} - \rho_{(x,y)}}{L+1}$$
(3)

$$j_{(x,y)}^{|} = D \frac{\rho_{(x,y+1)} - \rho_{(x,y)}}{L+1} \tag{4}$$

where ρ is the reservoir density of A particles. Using conservation of currents

$$j_{(x,y)}^{A} + j_{(x+1,y)}^{-} + j_{(x,y+1)}^{\dagger} = j_{(x,y)}^{-} + j_{(x,y)}^{\dagger}$$

$$\tag{5}$$

leads to a set of quadratic equations for the intersection densities $\rho_{(x,y)}$. For large L one of the two solutions reduces to a discrete Poisson equation.

$$\rho_{(x,y)} = \frac{1}{4} \left(\rho_{(x+1,y)} + \rho_{(x-1,y)} + \rho_{(x,y+1)} + \rho_{(x,y-1)} + \rho \right). \tag{6}$$

The other solution $\rho_{(x,y)} = 1$ demonstrates the fact that due to exclusion only one particle per site is allowed. (6) can be solved by use of the discrete sine transform $\tilde{\rho}_{(q,p)} = \sum_{x=1}^{N} \sum_{y=1}^{N} \rho_{(x,y)} \sin \frac{q\pi x}{N+1} \sin \frac{p\pi y}{N+1}$. We express (6) in terms of the transformed density $\tilde{\rho}_{(q,p)}$. Taking into account the boundary conditions $\rho_{0,y} = \rho_{x,0} = \rho_{x,N+1} = \rho_{N+1,y} = 0$ with $0 \le x, y \le N+1$ we find

$$\tilde{\rho}_{(q,p)} = \frac{2\rho}{\cos\frac{q\pi}{N+1} + \cos\frac{p\pi}{N+1} - 2} \sum_{n=1}^{N} \sum_{m=1}^{N} \sin\frac{q\pi n}{N+1} \sin\frac{p\pi m}{N+1}.$$
 (7)

The non zero contributions of the double sum can be expressed as a product of two Cotangens. Transforming back finally yields

$$\rho_{(x,y)} \equiv \rho M_{(x,y)} = -\frac{2\rho}{(N+1)^2} \sum_{n=1}^{N} \sum_{m=1}^{N} \frac{B_{(n,m)}}{(\cos\frac{n\pi}{N+1} + \cos\frac{m\pi}{N+1} - 2)} \sin\frac{n\pi x}{N+1} \sin\frac{n\pi y}{N+1}$$
(8)

$$B_{(n,m)} = \begin{cases} 0 & \text{if } n \text{ or } m \text{ even} \\ \cot \frac{m\pi}{2(N+1)} \cot \frac{n\pi}{2(N+1)} & \text{else} \end{cases}$$

$$(9)$$

However, similar to MTC in 2D [13], increasing the boundary density ρ eventually leads intersections to saturate starting from the most inner one. Thus, (8) is true only for small ρ . To be more precise (8) is a solution for $0 \le \rho \le \frac{1}{M([N+1]/2,[N+1]/2)}$. A further increase of ρ eventually leads other intersection to saturate. Fig. 3 shows the theoretical densities (system with N = 5-channels) as a function of ρ . We identify different regimes of saturating intersections. We observe a grouping $\{(1,1)\},\{(1,2),(1,3)\}$ and $\{(2,2),(2,3),(3,3)\}$ which is also supported by simulations (Fig. 4 same system size and slightly different model rates), where only intersections of the last group saturate. The smoothness of the simulated curves is due to finite-size effects which are not captured within mean field theory.

The situation is similar to the case in two dimensions. The main constrained of the MTC system becomes apparent as we consider large reactivities. The output is mainly determined

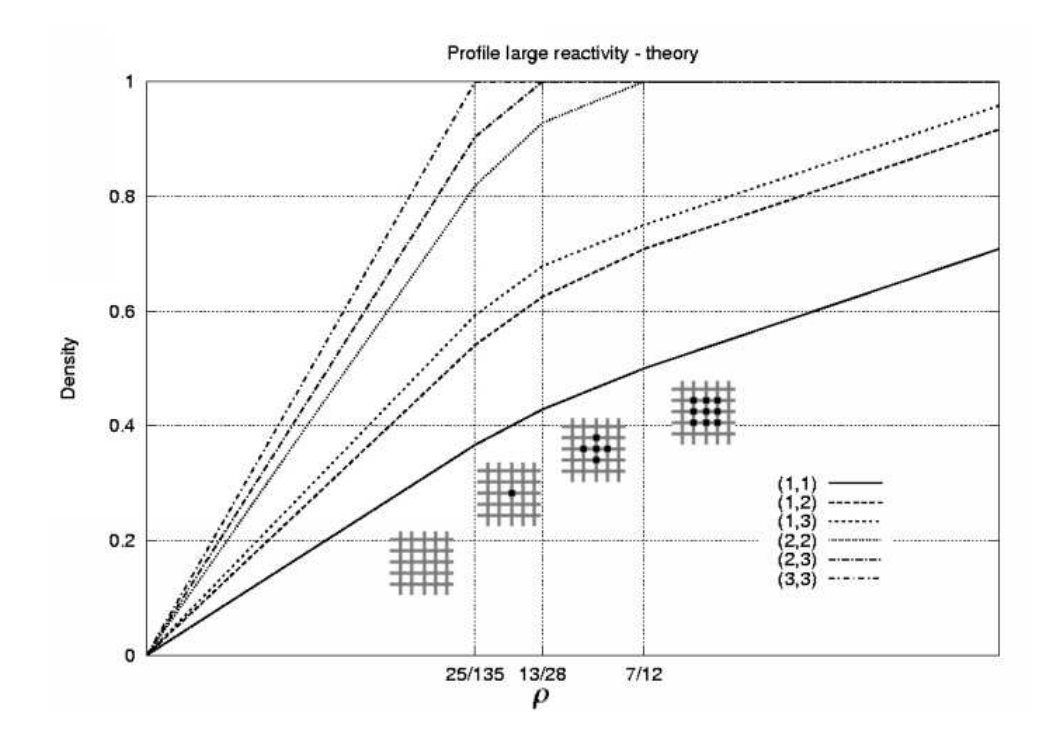


FIG. 3: Theoretical intersection densities for a lattice of N=5. The regimes of saturating intersections are indicated.

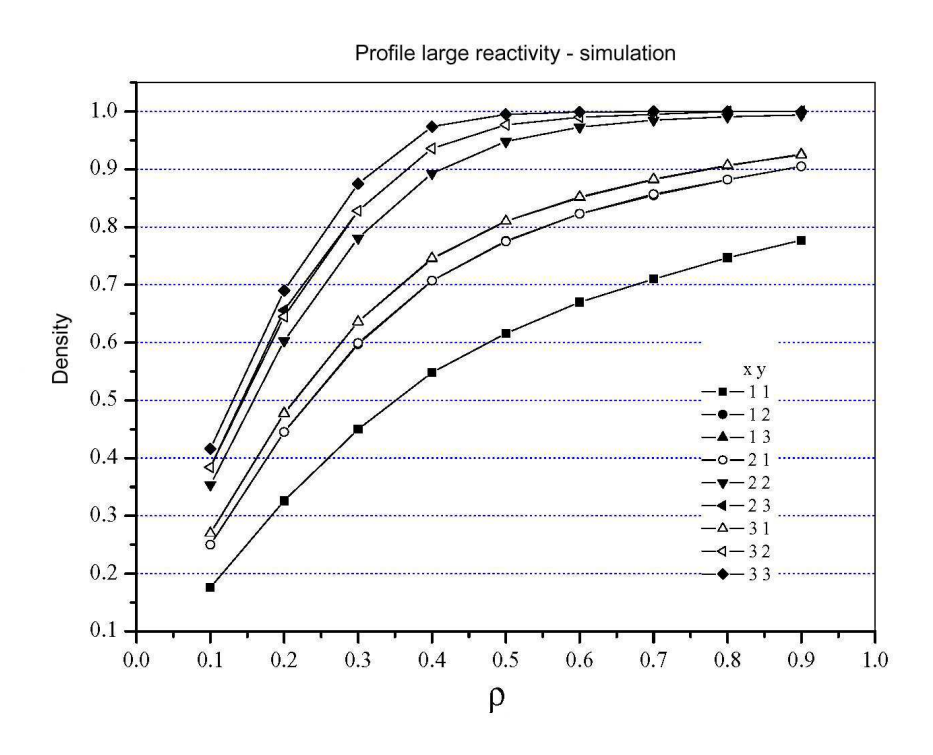


FIG. 4: Simulated intersection densities for a lattice of N=5 and L=10.

by two planes of β -channels. B particles leave the system through 8N channel segments. In the reference system the output is proportional to N^2 . Therefore a MTC effect is expected only for systems with small number of channels. Increasing the distance L would in principle favor MTC systems but reduces the absolute output. Simulations also show no evidence for a qualitative different picture compared to MTC in 2D.

For fixed moderate c this extreme situation is not realized, but nevertheless with increasing N one expects that the bulk gets increasingly depleted, since in each layer a fraction of A particles is converted into B particles. Thus fo lage N the total A-density in each layer may be described in a continuum desciption by the form

$$\frac{d}{dx}N_A(x) = -\gamma N_A(x) \tag{10}$$

for the number $N_A(x)$ of A-particles in layer x predicts an exponential decrease of the A density, leaving only an active boundary layer of finite thickness

$$\xi = 1/\gamma \propto 1/c \tag{11}$$

at the top and bottom respectively of the (in our simulation three-dimensional) grain. Hence, as a function of N, j_{MTC}^* saturates at some constant

$$\lim_{N \to \infty} j_{MTC}^*(c, N, L) = C_{MTC}^*(c, L).$$
 (12)

On the other hand, in the REF system the output current scales linearly with increasing N for all, even large, c. This is because even though again the bulk depletes with increasing N the active boundary layer is a surface scaling linearly with N. Thus

$$\lim_{N \to \infty} j_{REF}^*(c, N, L) = NC_{REF}^*(c, L)$$
(13)

Hence

$$R(c, N, L) \propto 1/N \tag{14}$$

and the MTC effect vanishes at some N for fixed reactivity c and channel length L.

IV. CONCLUSION

We have generalized the two-dimensional NBK-model for molecular traffic control to three space dimensions. We have focussed our attention on the case of short intersecting channels between catalytic centers which is the relevant setting from an applied perspective. Inspired by large deviation theory for nonequilibrium steady states and using exact results for the SEP we reduce the large number of freedom to a system of equations for the effective densities at the reaction sites. Our analytical treatment for large reactivities yields stationary density profiles which are supported by simulations. As in two dimensions [13] a sequence of surface induced saturations of the reaction sites inside the crystallite sets in. This leads to nonanalytical changes of the output of product molecules as a function of the input rate of reactands.

For moderate reactivities we obtain an exponentially decreasing loading as one probes the system further away from the boundary where reactands are adsorbed. The localization length is inversely proportional to the local reaction rate. As a consequence, the effective reactivity of crystallites with a diameter larger than the localization length does not scale with the surface area of the crystallite, but only with the diameter. Therefore, for moderate and high local reactivities and grain sizes currently used in industrial processes one expects no reaction enhancement through the MTC effect. However, as proposed in [23], nano-sized grains do exhibit this phenomenon and are thus potential candidates for exploiting MTC.

^[1] Ch. Baerlocher, W. M. Meier and D. H Olson, Atlas of Zeolite Structure Types, Elsevier: London 2001.

^[2] J. Kärger and D.M. Ruthven, Diffusion in Zeolites and Other Microporous Solids, Wiley: New York 1992.

^[3] E.G. Derouane and Z. Gabelica, J. Catal. 65 (1980) 486.

^[4] E.G. Derouane, Appl. Catal. A, N2 (1994) 115.

^[5] R. Q. Snurr and J. Kärger, Phys. Chem. B 101 (1997) 6469.

^[6] L. A. Clark, G. T. Ye, R. Q. Snurr, Phys. Rev. Lett. 84 (2000) 2893.

^[7] L. A. Clark, G. T. Ye, A. Gupta, L. L. Hall, R. Q. Snurr, J. Chem. Phys. 111 (1999) 1209.

^[8] M. Heuchel, R.Q. Snurr, E. Buss, Langmuir 13 (1997) 6249.

^[9] N. Neugebauer, P. Bräuer, J. Kärger, J. Catal. 194 (2000) 1.

^[10] J. Kärger, P. Bräuer, H. Pfeifer, Z. Phys. Chem. 104 (2000) 1707.

^[11] J. Kärger, P. Bräuer, A. Neugebauer, Europhys. Lett. 53 (2001) 8.

- [12] P. Bräuer, A. Brzank, J. Kärger, J. Phys. Chem. B 107 (2003) 1821.
- [13] A. Brzank, G. M. Schütz, P. Bräuer, and J. Kärger, Phys. Rev. E 69 (2004) 031102.
- [14] J.S. Beck, J.C. Vartulli, W.J. Roth, M.E. Leonowice, C.T. Kresge, K.D. Schmitt, C. T-W. Chu, D.H. Olsen, E.W. Sheppard, S.B. McCullen, J.B. Higgins, J.L. Schlenker, J. Am. Chem. Soc. 114 (1992) 10834.
- [15] J.H. Sun, Z. Shan, Th. Maschmeyer, M.-O. Coppens, Langmuir 19 (2003) 8395.
- [16] F. Spitzer, Adv. Math. 5 (1970) 246.
- [17] H. Spohn, J. Phys. A 16 (1983) 4275.
- [18] H. van Beijeren, K.W. Kehr, R. Kutner, Phys. Rev. B 28 (1983) 5711.
- [19] G. Schütz, S. Sandow, Phys. Rev. E 49 (1994) 2726.
- [20] T.M. Liggett: Stochastic Interacting Systems: Contact, Voter and Exclusion Processes (Springer, Berlin, 1999).
- [21] G.M. Schütz, in: *Phase Transitions and Critical Phenomena*, C. Domb and J. Lebowitz (eds.), (Academic, London, 2001).
- [22] C. Rödenbeck, J. Kärger, J. Chem. Phys. 110 (1999) 3970.
- [23] A. Brzank, G.M. Schütz, Appl. Catalysis A in press